Frontiers in Bioscience Landmark

Front. Biosci. (Landmark Ed) **2023**; 28(11): 303
https://doi.org/10.31083/j.fbl2811303

Original Research

Centrosomal Protein CEP135 Regulates the Migration and Angiogenesis of Endothelial Cells in a Microtubule-Dependent Manner

Kun Wang[1], Xin Wang[1], Fayun Zhao[1], Qiang Zhao[1], Shenke Kong[1], Peiyao Ma[1], Gang Wu[1], Wenzhi Wang[1], Xuejun Zhang[1,*]

[1]Department of Cardiology, Henan Provincial Chest Hospital, 450000 Zhengzhou, Henan, China
*Correspondence: zxj6817@126.com (Xuejun Zhang)
Academic Editor: Marcus Franz
Submitted: 25 July 2022 Revised: 19 November 2022 Accepted: 5 December 2022 Published: 27 November 2023

Abstract

Background: Angiogenesis is the formation of blood vessels by sprouting from mature blood vessels and is regulated by multiple factors; however, the role of centrosome and centrosomal proteins (CEP) in angiogenesis needs further study. centrosomal protein 135 (*CEP135*) is an important centrosome-associated protein that can affect a variety of cellular processes, such as the cell cycle, but its effect on angiogenesis is still unknown. **Methods**: Tube formation and *in vivo* angiogenesis assays were performed to confirm the effects of CEP135 on endothelial cell (EC) angiogenesis *in vitro* and in mice. Cell counting kit-8 (CCK-8), 3-(4,5-Dimethylthiazol-2-yl)-2,5-diphenyltetrazolium bromide (MTT), flow cytometry (FCM) and immunoblot assays were performed to confirm the effects of CEP135 on the proliferation and cell cycle of endothelial cells. Wound healing, transwell, and fluorescence staining were performed to confirm its effects on EC cell migration, polarization, and spindle orientation, and a tubulin turbidity assay was performed to confirm its effects on microtubule stabilization. **Results**: We conducted a series of experiments to explore the potential role of CEP135 in angiogenesis. CEP135 siRNA obviously inhibits angiogenesis *in vivo* compared with the control. CEP135 could mediate cell proliferation and the cell cycle by mediating spindle orientation. Moreover, we showed that CEP135 is involved in the regulation of angiogenesis by affecting the migration of endothelial cells using wound closure and transwell assays. We further demonstrated that CEP135 promotes endothelial polarization and microtubule stability, thus affecting cell migration. **Conclusions**: CEP135 was involved in the polarization of centrosomes, which is important for the migration of human umbilical vein ECs (HUVECs). These findings indicated that CEP135 may promote the polarization of HUVECs and accelerate migration, which in turn promotes angiogenesis.

Keywords: angiogenesis; CEP135; migration; polarization; endothelial cells

1. Introduction

Angiogenesis, which is the process relating to the formation of new blood vessels, is a highly dynamic process affecting degradation of the basement membrane, proliferation, directed migration of endothelial cells (ECs) and stabilization of new blood vessels [1,2]. Angiogenesis generally occurs in diverse physiological and pathophysiological processes and is mediated by the balance between a number of molecules, such as vascular endothelial growth factor (VEGF) [3,4]. During angiogenesis, proliferation and migration are critical and can promote the development of new blood vessels [5,6]. Although several studies have reported that centrosomes can affect numerous cell activities, there is little information regarding the association between centrosomes and the regulation of angiogenesis [5–7].

Centrosomes have been found in ECs; however, their function in blood vessels remains incompletely defined [8]. Centrosomes in ECs are known to be critical in blood vessel development [9]. In addition, ECs are highly responsive to blood flow, and centrosomes are involved in sensing fluid shear stress [10]. Endothelial centrosomes may also participate in vascular mural cell recruitment by activating the Notch pathway [11]. EC centrosomes have also been reported to be involved in the detection of shear forces during vascular development, which can affect the progression of atherosclerosis by the inhibition of proatherosclerotic signaling in the aorta [12]. Although centrosomes are widely involved in the formation and maintenance of blood vessels, their possible roles and the effects of multiple centrosomal proteins on angiogenesis are still unclear [13].

The centrosomal protein 135 (*CEP135*) gene encodes a centrosomal protein [14]. In addition, a *Bld10* mutant in *Chlamydomonas reinhardtii* has been shown to result in disorganized microtubules and the absence of basal bodies [15]. In cultured cells, CEP135 can localize to the cartwheel [16], and CEP135 has been reported to play a role in centriole biogenesis and particularly in central pair assembly [17]. Additionally, *CEP135* gene mutations have been shown to cause primary microcephaly in mice [17]. *CEP135* has also been shown to be amplified and mutated in aggressive breast tumor samples, suggesting that *CEP135* may serve as a potential candidate oncogene [17]. These previous findings indicated that CEP135 is critical in the functions of the centrosome; however, its possible effects on the angiogenesis of ECs remain unclear.

In the present study, CEP135 small interfering (si)RNA-transfected cells were used to reveal the role of CEP135 in angiogenesis, which was further investigated in nude mice. The present study provides novel insight into how centrosome proteins may regulate cell processes and reports a novel mechanism for the regulation of angiogenesis.

2. Materials and Methods

2.1 Cell Culture and Transfection

The experiments using primary human umbilical vein ECs (HUVECs) were approved by the Ethics Committee of the Chest Hospital of Henan Province (Zhengzhou, China). Primary HUVECs (cat. no. 8000) were obtained from ScienCell Research Laboratories, Inc., and cultured in RPMI-1640 medium supplemented with 10% FBS (both from Thermo Fisher Scientific, Inc., Waltham, MA, USA) and 1% penicillin and streptomycin in a 5% CO_2 incubator. All cell lines were validated by STR profiling and tested negative for mycoplasma. Cells were all cultured in a humidified incubator at 37 °C and 5% CO_2. Human CEP135 was cloned from a human cDNA library constructed using a SuperScript VILO™ cDNA kit (cat. no. 11754050; Thermo Fisher Scientific, Inc.). The RNA used for cDNA library construction was isolated from HUVECs. The CEP135 sequence was subcloned into pcDNA3.1 vectors (pcDNA3.1-Flag-CEP135; Addgene, Inc., Watertown, MA, USA) in our laboratory. The primers used for CEP135 cloning were as follows: forward 5′-CAAAATTATCTGCTGTGAAAGCTG-3′ and reverse 5′-CCAAAGCAACTGACAGTCG-3′. Plasmids were transfected into cells using Lipofectamine® 3000 (Invitrogen; Thermo Fisher Scientific, Inc.) according to the manufacturers' instructions. Human CEP135 and control siRNAs were synthesized by Guangzhou RiboBio Co., Ltd. (Guangzhou, China) and were transfected into HUVECs using Lipofectamine RNAiMAX reagent (Invitrogen; Thermo Fisher Scientific, Inc.). The sequences were as follows: siCEP135#1, 5′-UUUACAAGGAGUUCAUCACUCAGUC-3′; siCEP135#2, 5′-AUAACUUGUAGAGCAAGAUCUUCGC-3′; siControl (scrambled siRNA), 5′-UUAGGCGUACCUGACCAUGGAUUUC-3′.

The mouse CEP135 and control siRNAs were also synthesized by Guangzhou RiboBio Co., Ltd. and used to transfect mice during the *in vivo* angiogenesis assays. The sequences were as follows: siCEP135, 5′-CCAGCUGGGCUACCGCCAGA-3′; siControl (scrambled siRNA), 5′-AUUGCGUUACUAGGAUUUGGAUAUG-3′.

2.2 Antibodies and Reagents

Antibodies against γ-tubulin (cat. no. A302-630A) were purchased from Thermo Fisher Scientific, Inc., against α-tubulin (cat. no. sc-8035) were obtained from Santa Cruz Biotechnology, Inc., and against CEP135 (cat. no. ab75005), CDK4 (cat. no. ab108357) and cyclin D1 (cat. no. ab16663) were purchased from Abcam (Cambridge, UK). FITC- or TRITsC-conjugated secondary antibodies (cat. nos. ab6717, ab6718, ab6785 and ab6786) were obtained from Abcam. DAPI and Cell Counting Kit-8 (CCK-8) were purchased from Millipore Sigma (Burlington, MA, USA). MTT was purchased from Sangon Biotech Co. Ltd (Shanghai, China).

2.3 Angiogenesis in Vivo Assay

The experiment was performed according to a previous study [18]. All animal procedures were approved by the Institutional Animal Care and Use Committee of the Chest Hospital of Henan Province (approval no. IRM-DWLL-2020172). A total of eight female nude mice (age, 8 weeks; weight, 22–24 g; n = 4 mice/group) were purchased from Beijing Vital River Laboratory Animal Technology Co., Ltd. The experiment was performed according to a previous study [19]. The mice were sacrificed by cervical dislocation, and the lack of heartbeat was confirmed to validate death. The mice were monitored once a day before the experiment began and twice a day until the experiment ended.

Angiogenic capacity in mice was quantified with an *in vivo* angiogenesis assay kit (Trevigen, Inc., Gaithersburg, MD, USA). Angioreactors were filled with a small amount (20 µL) of basement membrane preparation premixed with angiogenic factors and filled with VEGF, heparin, and fibroblast growth factor-2 (FGF-2). Positive (only contains these factors) and negative controls (without these factors and siRNAs) were also set. The experimental groups included these factors and siRNAs. Mouse siRNAs at a final concentration of 2 µmol/L were then added to the angioreactors, and the transfection was finished 11 days after the transplant. The angioreactors were incubated for 1 h at 37 °C to induce gel formation and then implanted into the dorsal flank of 8-week-old nude mice. After 11 days, all of the mice were sacrificed by cervical dislocation, and the lack of heartbeat was confirmed to validate death. The angioreactors were ~5 mm long, and the mice had no adverse reactions after implantation. Cells were recovered from the angioreactors and stained with FITC-lectin at room temperature for 30 min, which stains EC glycoproteins. The relative fluorescence intensity was measured. The mRNA levels and density were calculated according to the average value of the 4 nude mice in each group.

2.4 RT-Quantitative (q)PCR

TRIzol® (cat. no. 15596026; Invitrogen; Thermo Fisher Scientific, Inc.) reagent was used to isolate RNA from HUVECs. Total RNA was reverse transcribed into cDNA at 42 °C for 1 h using M-MLV reverse transcriptase (cat. no. M1701; Promega Corporation, Madison, WI, USA). The $2^{-\Delta\Delta Ct}$ method was used to quantify the results [20]. The qPCR primers were designed

by Primer 5.0 software (PREMIER Biosoft, Palo Alto, CA, USA), and the sequences were as follows: GAPDH, forward 5′-CCAATGTGTCCGTCGTGGAT-3′ and reverse 5′-TGAAGTCGCAGGAGACAACC-3′; CEP135, forward 5′-TACTCCGCTCGGGAAAAACC-3′ and reverse 5′-TGCGCTGAAGTTCATCCCTT-3′.

2.5 Western Blot Analysis

HUVECs were lysed in a buffer containing 1% Triton X-100, 150 mM NaCl and 50 mM Tris (pH 7.5). Proteins were then transferred onto polyvinylidene difluoride membranes (Millipore Sigma), which were blocked at room temperature for 2 h in Tris-buffered saline containing 0.2% Tween 20 and 5% nonfat milk. The membranes were then incubated with antibodies against CEP135 (1:500; cat. no. ab75005; Abcam), CDK4 (1:500; cat. no. ab108357; Abcam), cyclin D1 (1:500; cat. no. ab16663; Abcam) and β-actin (1:2000; cat. no. ab8226; Abcam) for 2 h and with HRP-labeled secondary antibodies (cat. nos. ab6721 and ab6728, 1:3000; Abcam) for 45 min. Proteins were visualized using an enhanced chemiluminescence detection reagent (Pierce; Thermo Fisher Scientific, Inc.) and were analyzed.

2.6 Tube Formation Assay

HUVECs (10^5 per well) were plated onto 24-well plates precoated with Matrigel (1:1 diluted with serum-free medium) at 37 °C for 30 min. Images were captured after 3 and 6 h using an Axio Observer light microscope (Carl Zeiss AG). The tube length was measured using ImageJ 9.0 software (National Institutes of Health, Bethesda, MD, USA), and the node number was measured manually per field. The average tube length and node number were then calculated.

2.7 Fluorescence Microscopy and Image Analysis

For immunofluorescence microscopy, 10^5 HUVECs were grown on coverslips, fixed with 100% methanol at –20 °C for 20 min and blocked with 2% BSA (Millipore Sigma) in PBS for 20 min. Cells were incubated with the anti-α-tubulin and γ-tubulin antibodies (1:1000) for 2 h and then with FITC- or TRITC-labeled secondary antibodies (1:1000) for 2 h. DAPI was used for DNA staining for 3 min. Coverslips were then examined using a microscope and analyzed by ImageJ 9.0 software. The intensity of MT was measured by ImageJ software. We quantified MT fluorescence intensity per cell, measured 10 cells in each group, and took the average value.

2.8 3-(4,5-Dimethyl-2-Thiazolyl)-2,5-Diphenyl Tetrazolium Bromide (MTT) Assay

HUVECs were added to 96-well plates (1000 cells/well) and maintained for 48 h at 37 °C. Cells were subsequently treated with MTT agent for 4 h at 37 °C and washed with PBS. Formazan was then dissolved using 200 µL DMSO.

2.9 Cell Counting Kit-8 (CCK-8) Assay

HUVECs were plated in 96-well plates to a density of 1000 cells/well. Cells were then treated with CCK-8 for 4 h at 37 °C and measured at 450 nm wavelength.

2.10 Wound-Healing Assay

HUVECs transfected with siRNAs for 48 h were plated onto glass coverslips until 100% confluence. A 10-µL pipette tip was used to create a scratch, after which cells were washed twice with phosphate buffer saline (PBS) to remove cell debris and cultured in serum-free media for another 24 h. Images of the wound were captured using a light microscope at 0 and 24 h to determine the extent of wound closure using ImageJ 9.0 software, and the wound healing percentage was calculated as follows: Healing area/total area.

2.11 Cell Cycle Assay

The proportion of HUVECs (10^6) in different phases of the cell cycle (including G_1, S and G_2/M) was analyzed by flow cytometry. Briefly, 70% ethyl alcohol was used to fix HUVECs for 24 h at –20 °C. Subsequently, RNase A (10 mg/mL; cat. no. ST578; Beyotime, Shanghai, China) was used to incubate the cells for 10 min at 37 °C, and the cells were then incubated with 50 µg/mL propidium iodide (Abcam) at 37 °C for 30 min. Cell cycle progression was assessed using a FACSCalibur flow cytometer and CellQuest Pro 5.1 (BD Biosciences, Inc., Franklin Lakes, NJ, USA).

2.12 Transwell Assay

BD Falcon inserts (BD Biosciences, Inc., NJ, USA) were used as upper chambers, and 24-well plates were used as lower chambers. Cell culture inserts were coated with 50 µL 20% Matrigel at 37 °C for 30 min. Subsequently, 10^5 HUVECs/well transfected with siRNAs were placed in the upper chamber (serum-free medium), and complete medium was added to the lower chamber. Invaded cells on the underside were fixed with 4% paraformaldehyde for 25 min and stained with crystal violet (2%) solution for 25 min, and images were captured using a microscope.

2.13 Cell Polarization and Tubulin Stabilization Assay

HUVECs transfected with siRNAs for 48 h were plated and grown onto coverslips until 100% confluence. The HUVEC monolayer was scratched; 3 h after scratching, the cells were fixed with 4% paraformaldehyde for 30 min.

For tubulin stabilization assays, HUVECs were placed on ice for 0 and 30 min for depolymerization, followed by immunofluorescence detection of morphology after fixing the cells were fixed with 4% paraformaldehyde for 30 min.

Microtubules (green), centrosomes (red) and nuclei (blue) were stained with α-tubulin and γ-tubulin antibodies (1:1000) for 2 h at room temperature and then with secondary antibodies (1:1000) for 2 h. Subsequently, slides

were stained with DAPI (1:3000) for 3 min. Coverslips were mounted with 90% glycerol in PBS and then examined. Border cells with the microtubule organizing center (MTOC) situated between the nucleus and the leading edge were considered polarized using ImageJ 9.0 software.

2.14 Tubulin Turbidity Assay

Tubulin (5 mg/mL; Cytoskeleton, Inc., California, USA) and purified His-CEP135 proteins (100 nM; Guidechem, Nanjing, China) were added to a 96-well plate on ice and then transferred to a spectrophotometer. The polymerization was monitored by measuring the absorbance (350 nm). Spontaneously assembled microtubules with or without His-CEP135 (100 nM) at 37 °C were diluted with PBS, followed by shifting the temperature from 20 °C to 4 °C, according to a previous study [21].

2.15 Statistical Analysis

Data were analyzed using GraphPad 8.0 software (GraphPad Software, Inc., La Jolla, CA, USA). Error bars represent the mean ± SEM. The unpaired Student's *t* test was used to determine statistical significance between two groups. One-way ANOVA followed by Tukey's post hoc test was used for multiple comparisons. $p < 0.05$ was considered statistically significant.

3. Results

3.1 CEP135 is Essential for Angiogenesis

To investigate whether CEP135 is essential for angiogenesis, the present study examined the effect of CEP135 siRNAs on vascular endothelial tube formation *in vitro*. Two different siRNAs were used to target the CDS region of CEP135 mRNA and therefore induce the knockdown of CEP135, and both were able to effectively knockdown CEP135 expression in HUVECs (Fig. 1A,B). After plating cells for 3 or 6 h, a tubular network of interconnecting branches was observed in the control siRNA group; in contrast, fewer tubes were detected in the CEP135 siRNA groups (Fig. 1C). The accumulated tube length and node numbers at 3 h were measured as an index of angiogenesis (Fig. 1D,E). In addition, a CEP135 overexpression plasmid was transfected into HUVECs, and its efficiency was confirmed by western blotting (**Supplementary Fig. 1**). CEP135 overexpression had modest effects on the angiogenesis of HUVECs, with only slight changes in tube length and node numbers (Fig. 1F,G and **Supplementary Fig. 2**). However, overexpression of CEP135 rescued the inhibition of angiogenesis in HUVECs caused by CEP135 knockdown (Fig. 1H,I). These findings indicated that CEP135 was essential for angiogenesis.

3.2 CEP135 Knockdown Impairs Angiogenesis in Mice

To verify the effects of CEP135 on HUVEC angiogenesis *in vitro*, the present study assessed the effect of CEP135 on angiogenesis in a mouse model using semiopen angioreactors that were filled with extracellular matrix-containing angiogenic factors implanted into 4 nude mice per group (Fig. 2A). A total of 12 days after implantation, the silencing efficiency of siCEP135 was detected by qPCR (Fig. 2B). Vascular structures were identified in the angioreactors (Fig. 2C, positive control), whereas no vascular structures were detected in angioreactors without any angiogenic factors (Fig. 2C, negative control).

Notably, CEP135 ablation in the angioreactors markedly inhibited new vascular growth induced by heparin, VEGF and FGF-2, whereas control siRNA had no effect on vascular growth into the angioreactors (Fig. 2C). To examine the angiogenic level *in vivo*, the vascular density was assessed and was shown to be significantly decreased in the CEP135 siRNA-treated group (Fig. 2D). Subsequently, the cells were removed from the angioreactors and stained with FITC-lectin, an EC marker. As shown in Fig. 2E, the fluorescence intensity of cells in the siCEP135 group was significantly decreased compared with the control ($p < 0.05$), suggesting that CEP135 depletion *in vivo* could markedly inhibit angiogenesis. These findings confirmed an important role for CEP135 in angiogenesis *in vivo*.

3.3 CEP135 Knockdown Suppresses HUVEC Proliferation and Cell Cycle Progression

Since CEP135 affected EC angiogenesis, its effects on the proliferation of HUVECs were assessed. Through CCK-8 and MTT assays, it was demonstrated that CEP135 knockdown markedly suppressed the proliferation and survival of ECs, as indicated by a decreased optical density value (Fig. 3A,B). These results indicated that CEP135 knockdown inhibited cell proliferation. Subsequently, the effects of CEP135 on cell cycle progression were analyzed by flow cytometry. Notably, CEP135 knockdown led to cell cycle arrest (Fig. 3C and **Supplementary Fig. 3**). In addition, the protein expression levels of CDK4 and cyclin D1, two markers of the cell cycle, were decreased following CEP135 knockdown in ECs (Fig. 3D–F; $p < 0.05$). These findings indicated that CEP135 ablation suppressed HUVEC proliferation and cell cycle progression.

3.4 CEP135 Knockdown Leads to Defects in Spindle Orientation in ECs

CEP135 is a centrosomal protein that has the potential to affect mitosis [15]. Therefore, the present study measured the effects of CEP135 on cell division. Spindle orientation is important for many developmental processes, including cell division, epithelial tissue homeostasis and regeneration. Spindle orientation was determined by measuring the angle between the spindle axis and the substratum. Notably, knockdown of CEP135 resulted in an increase in spindle angle, indicative of defective spindle orientation, whereas spindle length was not affected (Fig. 4A–E). The model was shown in Fig. 4A. These findings suggested that CEP135 depletion led to defects in spindle orientation in ECs.

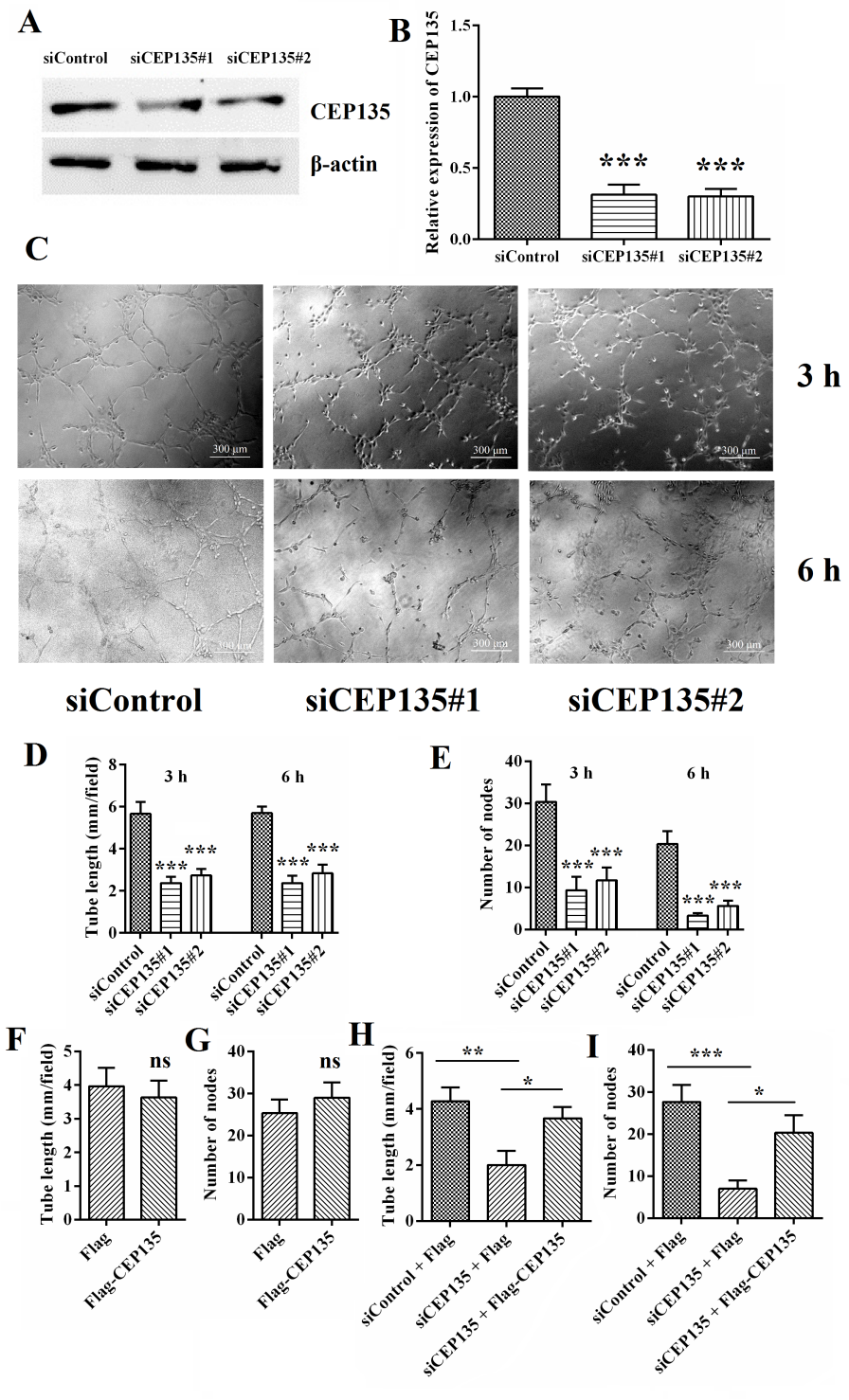

Fig. 1. CEP135 depletion leads to angiogenic defects in HUVECs. (A,B) Western blot analysis of CEP135 and β-actin expression in HUVECs transfected with siCEP135 or siControl for 24 h. (C) HUVECs transfected with siCEP135 or siControl were plated onto Matrigel, and images were captured after 3 and 6 h. (D) Tube lengths and (E) node numbers were measured at 3 and 6 h. (F–I) HUVECs transfected with the indicated siRNAs or plasmids were plated onto Matrigel, and images were captured after 6 h. (F,H) Tube lengths and (G,I) node numbers were measured after 6 h. (B,D,E) Data were analyzed using one-way ANOVA. (F–I) Data were analyzed using unpaired Student's *t* test. Error bars indicate SEM. $^{*}p < 0.05$, $^{**}p < 0.01$, $^{***}p < 0.001$, as indicated or vs. siControl. Scale bar, 300 μm. Each assay was performed 3 times. ns, not significant; CEP135, centrosomal protein 135; si/siRNA, small interfering RNA; HUVECs, human umbilical vein endothelial cells.

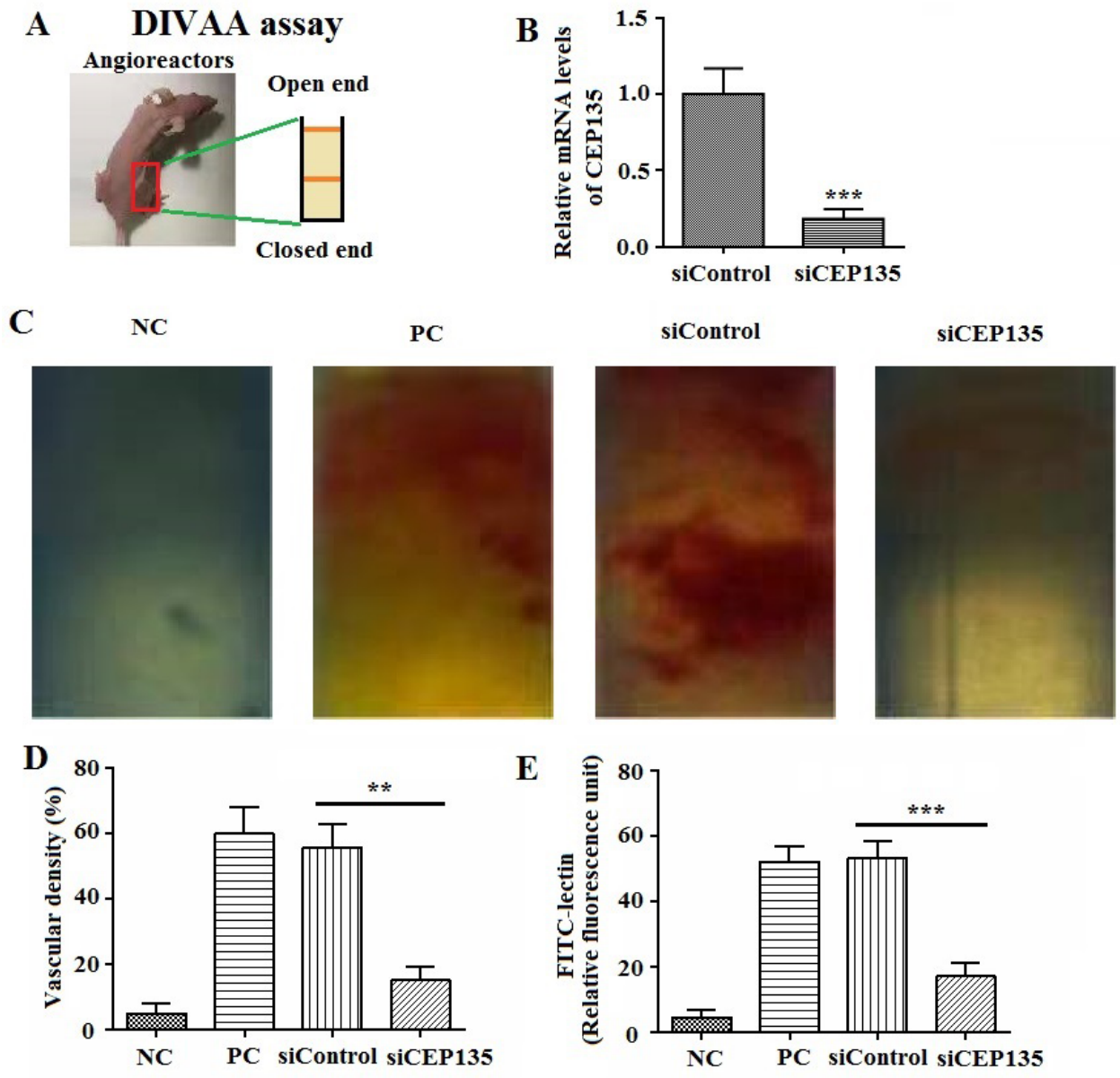

Fig. 2. CEP135 knockdown leads to angiogenic defects *in vivo*. (A) Representative image of an athymic nude mouse with a semiclosed angioreactor. (B) The efficiency of CEP135 knockdown was measured through quantitative PCR. (C) Vascular growth for 12 days. In siRNA experiments, siCEP135 or siControl. (D) Vascular density and (E) angiogenic responses were semiquantified by FITC-lectin staining. Error bars indicate SEM. $^{**}p < 0.01$, $^{***}p < 0.001$, as indicated or vs. siControl. N = 4 for each group. CEP135, centrosomal protein 135; si/siRNA, small interfering RNA; NC, negative control; PC, positive control; DIVAA, directed *in vivo* angiogenesis assay.

3.5 CEP135 is Essential for HUVEC Migration and Polarization

The present study then assessed the effect of CEP135 on HUVEC migration. A HUVEC monolayer was scratched with a pipette tip, and closure of the wounded area was documented to evaluate the capacity of cell migration. The wounded area in the control group was fully recovered after 24 h as a consequence of directed cell migration (Fig. 5A,B), suggesting the effects on cell migration. Transwell assays also revealed that CEP135 knockdown suppressed the invasion of HUVECs (Fig. 5C,D).

Polarization is a critical step in cell migration that involves the rearrangement of microtubules and reorientation of the centrosome [15]. HUVECs transfected with control or CEP135 siRNAs were scratched, and the cells were fixed 3 h later. In the control siRNA group, cells at the wound margin demonstrated a typical polarized structure, with the centrosome positioned between the nucleus and the leading edge (Fig. 6A,B). In contrast, the polarized morphology was suppressed in cells from the siCEP135 group (Fig. 6A). By semiquantifying the percentage of polarized cells, it was revealed that knockdown of CEP135 expression significantly

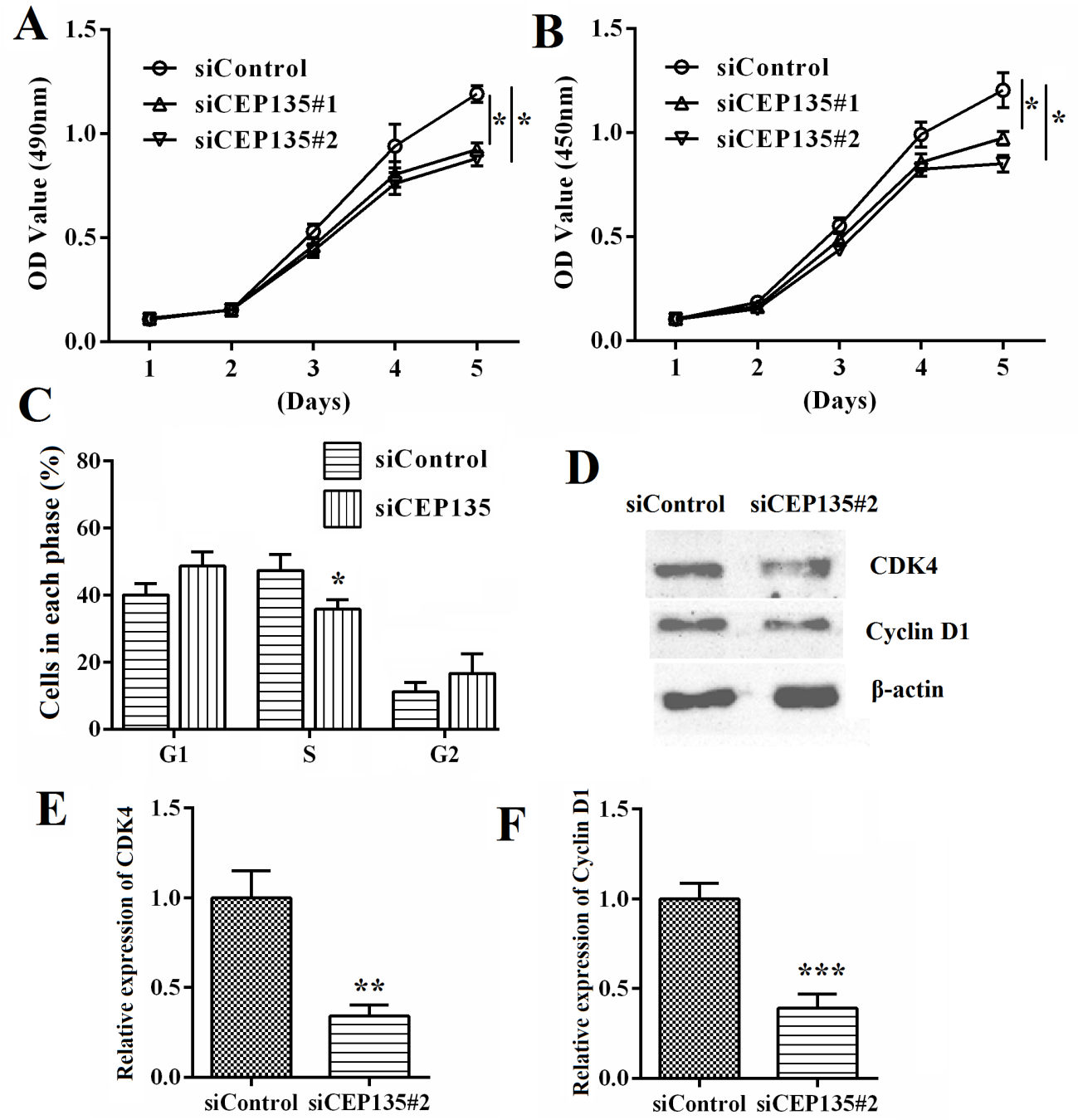

Fig. 3. CEP135 knockdown suppresses HUVEC proliferation and cell cycle progression. (A) MTT and (B) Cell Counting Kit-8 assays revealed the effects of CEP135 on the proliferation of HUVECs posttransfection. (C) Flow cytometry showed the effect of CEP135 on the cell cycle progression of HUVECs posttransfection with the transfection of control and human CEP135 siRNA#1, and the percentage of cells at different stages of the cell cycle was analyzed. (D) Western blot analysis showed the effects of CEP135 on the expression levels of (E) CDK4 and (F) Cyclin D1 upon transfection with control and CEP135 siRNA#1. Each assay was performed 3 times. One-way ANOVA was used for hypothesis testing for significance in A and B. Error bars indicate SEM. $^{*}p < 0.05$, $^{**}p < 0.01$, $^{***}p < 0.001$ vs. siControl.

inhibited cell polarization (Fig. 6C,D). In addition, the results indicated that CEP135 was critical for HUVEC migration and polarization by affecting the polarization angles (Fig. 6D).

3.6 CEP135 Influences Microtubule Stabilization

The present study assessed the mechanism underlying the effects of CEP135 on EC proliferation and migration. The present study investigated whether CEP135 was involved in the regulation of microtubule stabilization, which

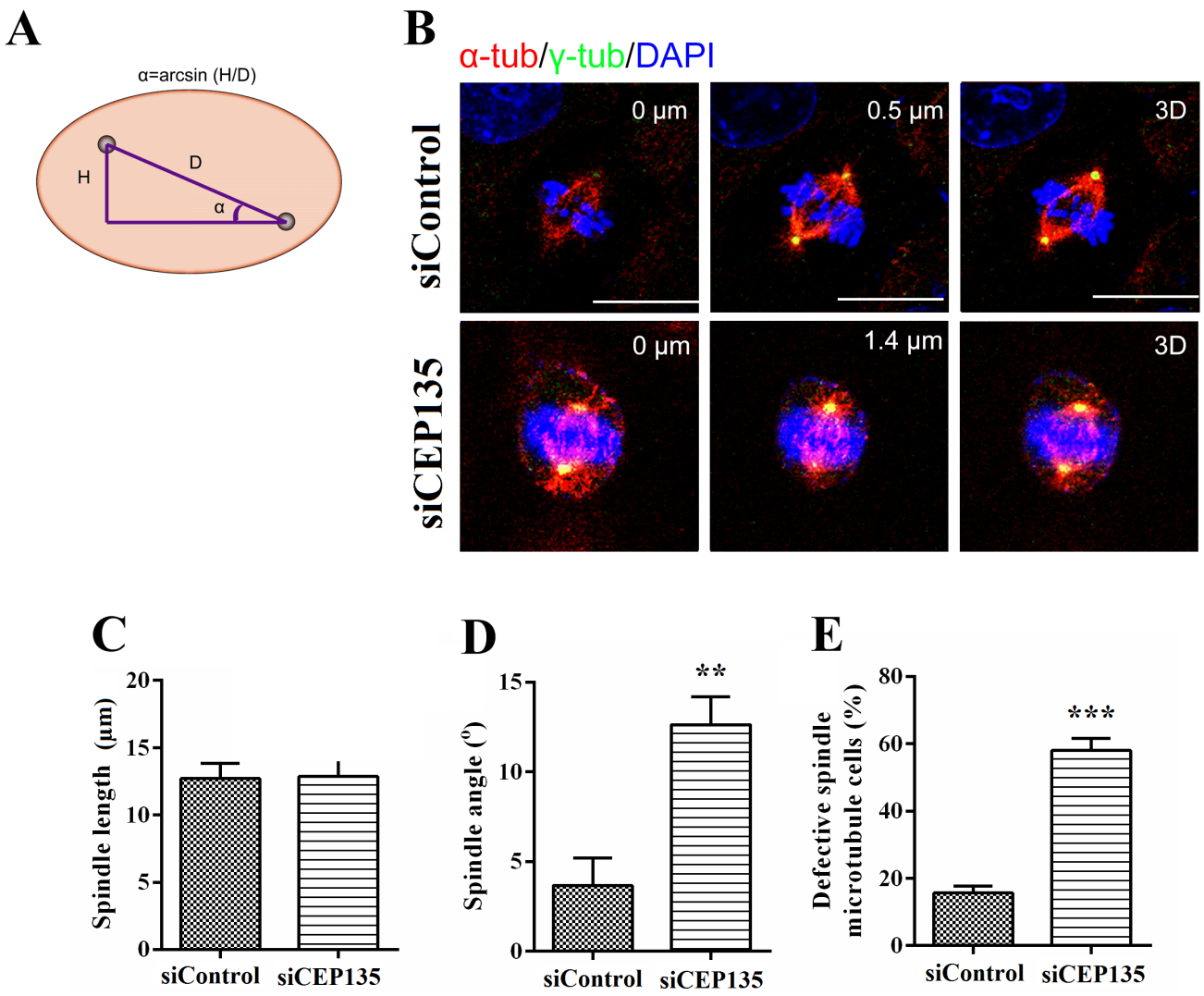

Fig. 4. CEP135 knockdown affects the spindle orientation of HUVECs. (A) Scheme depicting spindle angle (α) measurement. (B) Representative immunostaining images, (C) average spindle length, (D) average spindle angle and (E) percentage of cells with long astral microtubules. The position of the z stage is indicated in micrometers; 3D, xy projection. Cell numbers: N = 10 for each group. Error bars indicate SEM. Data were analyzed using unpaired Student's *t* test. Scale bar, 5 μm. $^{**}p < 0.01$, $^{***}p < 0.001$ vs. siControl.

is critical for cell polarization and migration. CEP135 knockdown significantly inhibited microtubule stabilization when cells were placed on ice for 30 min (Fig. 7A,B; $p < 0.05$). To examine whether CEP135 directly regulates microtubule stability, tubulin polymerization was assessed using an *in vitro* tubulin turbidity assay. CEP135 was shown to increase tubulin turbidity (Fig. 7C) and protected the microtubules from dilution- and cooling-induced disassembly (Fig. 7D). Taken together, these findings indicated that CEP135 may influence microtubule stabilization via the regulation of microtubule rearrangement in ECs.

4. Discussion

Angiogenesis refers to the process of sprouting of new blood vessels from existing vessels, which is regulated by a number of proangiogenic and inhibitory factors [4]. In adults, angiogenesis is virtually nonexistent [4]. This process often occurs in pathological processes, such as retinopathy of prematurity, tumor development and metastasis. Despite some understanding of angiogenesis, the relationship between centrosomes and endothelial angiogenesis is still poorly understood [7]. At present, some proteins that can be located in the centrosome, such as CEP70, have been reported to promote angiogenesis, and an in-depth understanding of this process is helpful to further reveal the pathogenesis of angiogenesis and related diseases [22]. The present study revealed that a centrosomal protein, CEP135, could serve as a regulator of angiogenesis.

Centrosomal proteins have multiple cellular functions in ECs [23]. They can mediate several microtubule-related processes, such as migration and directed cell division, by mediating microtubule dynamics and stabilization [8].

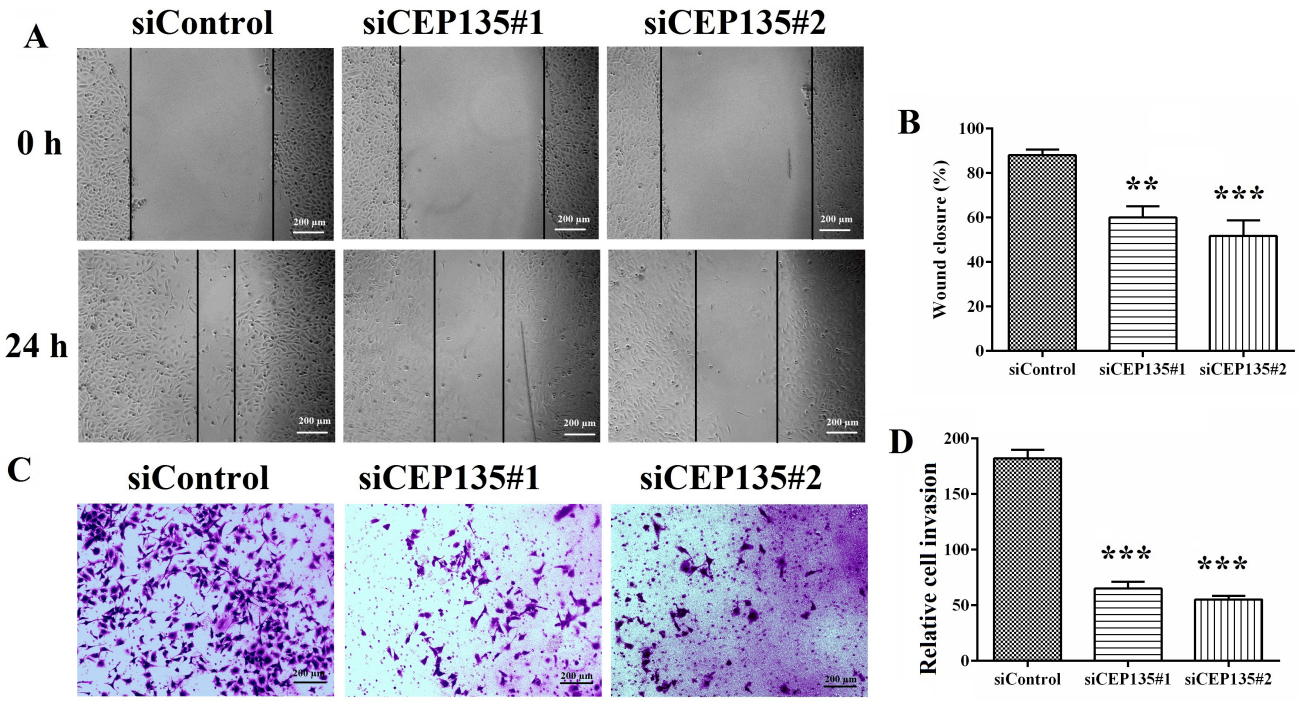

Fig. 5. CEP135 is critical for vascular endothelial cell migration. (A) HUVECs transfected with siControl or siCEP135 were scratched, and images of the wound margins were captured after 0 and 24 h. (B) The extent of wound closure was semiquantified by measuring the wound area. (C) Cells invading the underside of the insert were stained with crystal violet. (D) Semiquantification of the number of invaded cells. Data were analyzed using one-way ANOVA. Error bars indicate SEM. Scale bar, 200 μm. $^{**}p < 0.01$, $^{***}p < 0.001$ vs. siControl. Each assay was performed 3 times. CEP135, centrosomal protein 135.

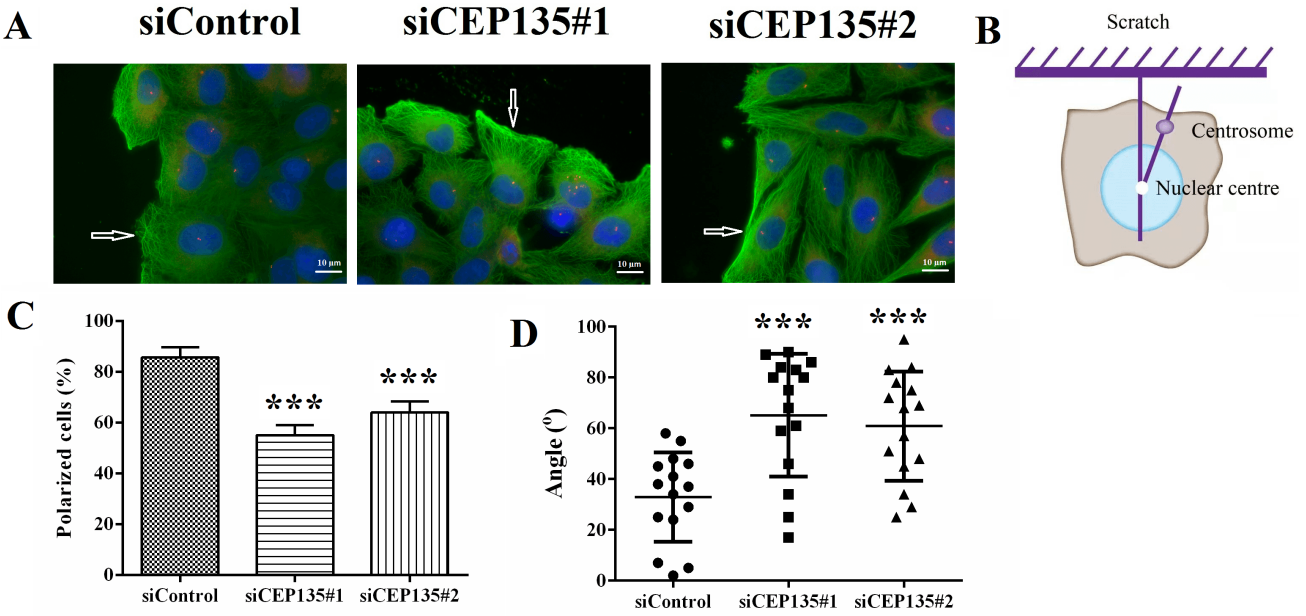

Fig. 6. CEP135 mediates vascular endothelial cell polarization. (A) Immunofluorescence microscopy images of siControl- and siCEP135-transfected HUVECs. α-Tubulin (green) and γ-tubulin (red) staining showed polarization defects. The arrows indicate the polarization of HUVECs. (B) A model showing the measurement of the angle of polarization of cells. The (C) percentage and (D) angle of polarized cells were affected by siCEP135. Data were analyzed using one-way ANOVA. Error bars indicate SEM. Scale bar, 10 μm. Cell numbers: N = 10 for each group. $^{***}p < 0.001$ vs. siControl.

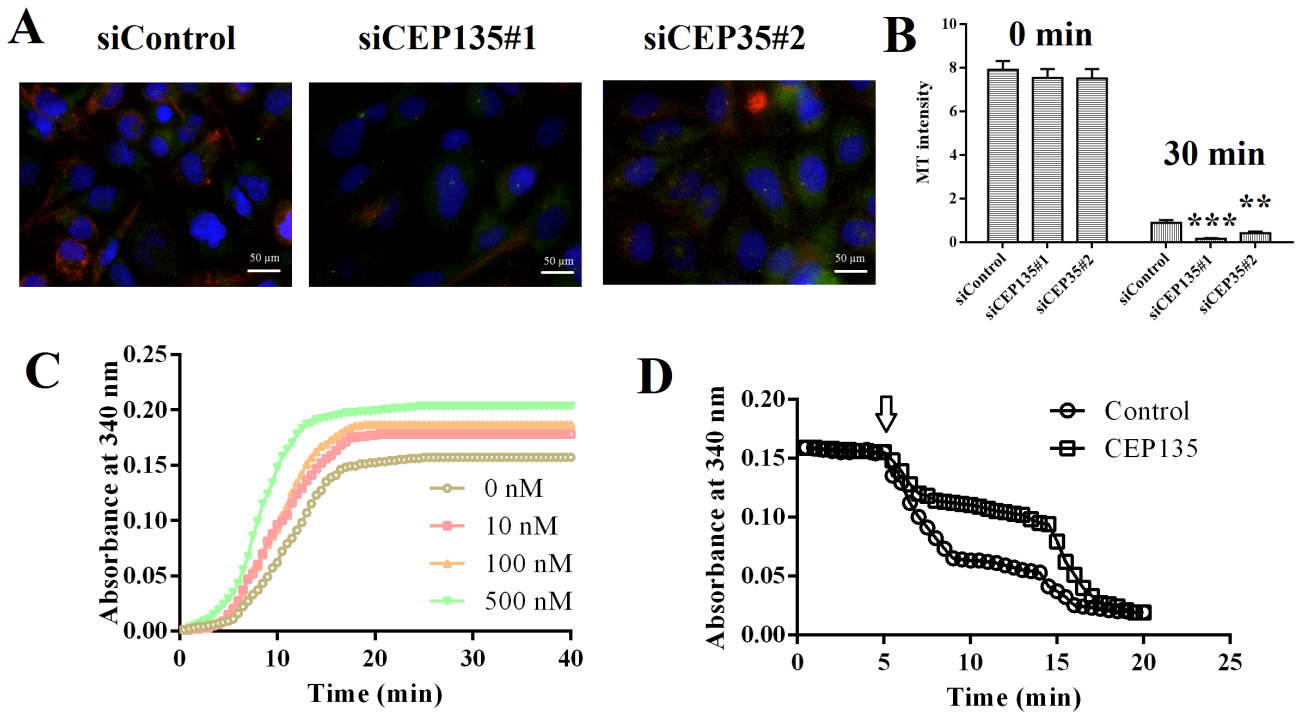

Fig. 7. CEP135 is critical for vascular endothelial cell MT stabilization. (A) Immunofluorescence microscopy images of siControl- and siCEP135-transfected HUVECs. α-Tubulin (green) and γ-tubulin (red) staining showed the MT stabilization of HUVECs on ice for 30 min. (B) Semiquantitative immunofluorescence. Cell numbers: N = 10 for each group. (C) Effects of purified CEP135 proteins (0, 10, 100 and 500 nM) on tubulin polymerization continuously measured for 40 min at a 350 nm wavelength at intervals of 30 sec. (D) MT depolymerization upon dilution and cooling was measured at a 350 nm wavelength. The arrow refers to the dilution time point. Data were analyzed using one-way ANOVA. Error bars indicate SEM. Scale bar, 50 μm. $^{**}p < 0.01$, $^{***}p < 0.001$ vs. siControl. Each assay was performed 3 times. CEP135, centrosomal protein 135; si, small interfering RNA; HUVECs, human umbilical vein endothelial cells; MT, microtubule.

The present study demonstrated that a centrosomal protein, CEP135, could serve as a regulator of angiogenesis. Through *in vitro* and *in vivo* assays, it was demonstrated that knockdown of CEP135 suppressed HUVEC angiogenesis. Further *in vitro* assays showed that CEP135 knockdown suppressed HUVEC proliferation and cell cycle progression, possibly via alterations to the spindle. In addition, knockdown of CEP135 inhibited cell migration by mediating cell polarization. Furthermore, CEP135 was revealed to mediate microtubule stabilization, thereby mediating cell migration, proliferation and angiogenesis of HUVECs (Fig. 8). It was therefore hypothesized that CEP135 could serve as a promising angiogenic regulator.

The role of CEP135 in multiple cellular processes has been well documented [16,17]. For example, depletion of CEP135 has been reported to lead to a disorganized interphase and multiple and fragmented centrosomes with disorganized microtubules [24]. Similarly, the present study revealed that the knockdown of CEP135 led to decreased microtubule stabilization in HUVECs and that several microtubule-dependent cellular processes were further affected. The knockdown of CEP135 has been revealed to suppress cell division and cause disordered neuronal cell polarity, which is essential for neuronal migration [25]. Similarly, the present study also revealed the effects of CEP135 on HUVEC polarization. Furthermore, mutations in CEP135 were reported to cause primary microcephaly and subcortical heterotopia in a microtubule-dependent manner [24]. Other studies have also revealed the multiple cellular functions of CEP135. A homozygous *CEP135* mutation was revealed to be associated with multiple morphological abnormalities of the sperm flagella [17]. In addition, CEP135 was shown to be required to establish centrosome asymmetry in *Drosophila* neuroblasts [26]. All these previous studies have confirmed that CEP135 could serve as a promising target for the treatment of multiple diseases.

The present study also revealed the effects of CEP135 on the regulation of microtubule stabilization. A previous study indicated that CEP135 contains a two-stranded coiled-coil domain, which is critical for microtubule binding [27]. A previous study indicated that the loss-of-function mutation of CEP135 limited the localization of other centrosomal proteins, including SAS-6, CPAP and γ-tubulin [16]. This previous study also revealed that CEP135 isoforms were differentially regulated during the cell cy-

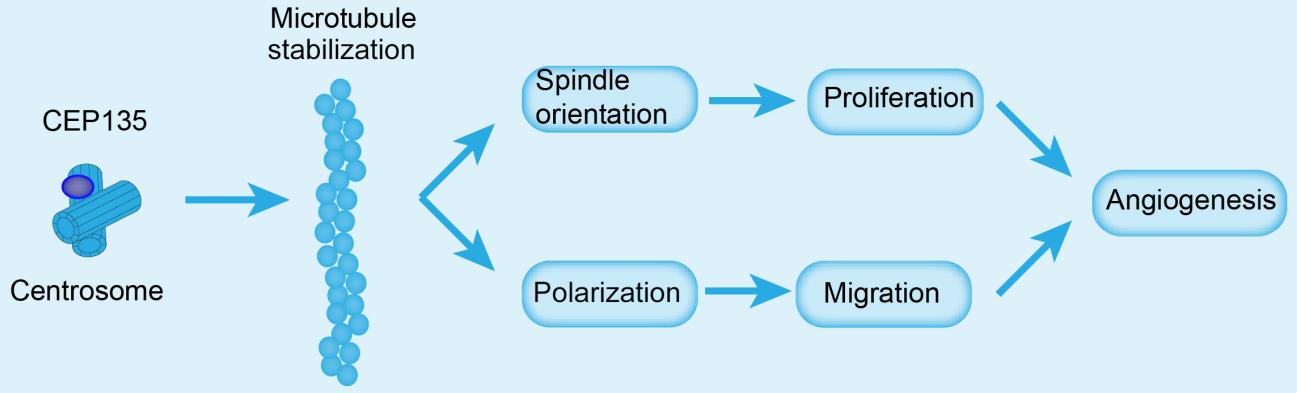

Fig. 8. Molecular model for the role of CEP135 in angiogenesis. CEP135 was involved in the polarization of centrosomes, which is important for HUVEC migration. These findings indicated that CEP135 may promote the polarization of HUVECs and accelerate migration, which in turn promotes angiogenesis. CEP135, centrosomal protein 135; HUVECs, human umbilical vein endothelial cells.

cle. Centrosome amplification after hydroxyurea treatment could also increase significantly in CEP135-knockdown cells, suggesting an inhibitory role for the protein in centrosome reduplication during S-phase arrest [28]. Notably, the present study revealed that knockdown of CEP135 led to cell cycle arrest in HUVECs and a decrease in S-phase cells.

Several studies have indicated the effects of centrosome- or microtubule-related proteins on angiogenesis; however, to the best of our knowledge, the present study is the first to demonstrate that the centrosomal protein CEP135 could affect the angiogenesis of HUVECs by mediating proliferation and migration in a microtubule-dependent manner [29,30]. Through *in vitro* assays, it was revealed that CEP135 mediated HUVEC angiogenesis by mediating proliferation and migration. Similarly, the *in vivo* assays confirmed its effects on angiogenesis.

Notably, cell polarization is the most important link in the early stage of cell migration and is mainly regulated by MTOCs and microtubules. After cell polarization, the microtubules rearrange, resulting in the movement of intracellular substances in the direction of migration through the microtubules [29,30]. Therefore, the present study assessed the effect of CEP135 on cell polarization and confirmed its effect on migration.

CEP135, as a centrosomal protein, plays an important role in centrosomes and MTOCs and participates in the regulation of microtubule stability. Due to the effect of CEP135 on microtubule-related functions, HUVEC proliferation and migration are further affected, both of which are regulated by microtubules.

5. Conclusions

In conclusion, the present study revealed that CEP135 mediated the angiogenesis of HUVECs *in vitro* and in mice. CEP135 regulated cell proliferation and migration by mediating spindle orientation and cell polarization. Furthermore, the effects of CEP135 on the stabilization of microtubules were confirmed. The present study indicated the role of CEP135 in angiogenesis and that it could serve as a critical regulator during the process of angiogenesis.

Availability of Data and Materials

Additional supporting information may be found in the online version of the article at the publisher's website. And the datasets used and/or analyzed during the present study are available from the author on reasonable request.

Author Contributions

KW, XW, FZ and XZ carried out molecular biology experiments and drafted the manuscript. KW, QZ, SK and PM designed the study and performed statistical analysis. KW, GW, WW and XZ conceived the study, participated in its design, coordinated the study and drafted the manuscript. KW and XZ confirm the authenticity of all the raw data. All authors contributed to editorial changes in the manuscript. All authors have read and approved the final manuscript.

Ethics Approval and Consent to Participate

All animal procedures were approved by the Institutional Animal Care and Use Committee of the Chest Hospital of Henan Province (approval no. IRM-DWLL-2020172).

Acknowledgment

Not applicable.

Funding

This research received no external funding.

Conflict of Interest

The authors declare no conflict of interest.

Supplementary Material

Supplementary material associated with this article can be found, in the online version, at https://doi.org/10.31083/j.fbl2811303.

References

[1] Heydari S, Kashani L, Noruzinia M. Dysregulation of Angiogenesis and Inflammatory Genes in Endometrial Mesenchymal Stem Cells and Their Contribution to Endometriosis. Iranian Journal of Allergy, Asthma, and Immunology. 2021; 20: 740–750.

[2] Li J, Zhao Y, Zhu W. Targeting angiogenesis in myocardial infarction: Novel therapeutics (Review). Experimental and Therapeutic Medicine. 2022; 23: 64.

[3] Mocanu C. Mechanism of angiogenesis. Ocular involvement. Oftalmologia. 2003; 59: 3–8.

[4] Kretschmer M, Rüdiger D, Zahler S. Mechanical Aspects of Angiogenesis. Cancers. 2021; 13: 4987.

[5] Jeong H, Choi D, Oh Y, Heo J, Hong J. A Nanocoating Co-Localizing Nitric Oxide and Growth Factor onto Individual Endothelial Cells Reveals Synergistic Effects on Angiogenesis. Advanced Healthcare Materials. 2022; 11: e2102095.

[6] Liu Y, Tian Y, Guo Y, Yan Z, Xue C, Wang J. DHA-enriched phosphatidylcholine suppressed angiogenesis by activating PPARγ and modulating the VEGFR2/Ras/ERK pathway in human umbilical vein endothelial cells. Food Science and Biotechnology. 2021; 30: 1543–1553.

[7] Martin M, Veloso A, Wu J, Katrukha EA, Akhmanova A. Control of endothelial cell polarity and sprouting angiogenesis by non-centrosomal microtubules. eLife. 2018; 7: e33864.

[8] Kushner EJ, Ferro LS, Liu J, Durrant JR, Rogers SL, Dudley AC, *et al*. Excess centrosomes disrupt endothelial cell migration via centrosome scattering. The Journal of Cell Biology. 2014; 206: 257–272.

[9] Ricolo D, Deligiannaki M, Casanova J, Araújo SJ. Centrosome Amplification Increases Single-Cell Branching in Post-mitotic Cells. Current Biology. 2016; 26: 2805–2813.

[10] Iomini C, Tejada K, Mo W, Vaananen H, Piperno G. Primary cilia of human endothelial cells disassemble under laminar shear stress. The Journal of Cell Biology. 2004; 164: 811–817.

[11] Vladar EK, Stratton MB, Saal ML, Salazar-De Simone G, Wang X, Wolgemuth D, *et al*. Cyclin-dependent kinase control of motile ciliogenesis. eLife. 2018; 7: e36375.

[12] Haust MD. Endothelial cilia in human aortic atherosclerotic lesions. Virchows Archiv. A, Pathological Anatomy and Histopathology. 1987; 410: 317–326.

[13] Buglak DB, Kushner EJ, Marvin AP, Davis KL, Bautch VL. Excess centrosomes disrupt vascular lumenization and endothelial cell adherens junctions. Angiogenesis. 2020; 23: 567–575.

[14] Carvalho-Santos Z, Machado P, Alvarez-Martins I, Gouveia SM, Jana SC, Duarte P, *et al*. BLD10/CEP135 is a microtubule-associated protein that controls the formation of the flagellum central microtubule pair. Developmental Cell. 2012; 23: 412–424.

[15] Mottier-Pavie V, Megraw TL. Drosophila bld10 is a centriolar protein that regulates centriole, basal body, and motile cilium assembly. Molecular Biology of the Cell. 2009; 20: 2605–2614.

[16] Dahl KD, Sankaran DG, Bayless BA, Pinter ME, Galati DF, Heasley LR, *et al*. A Short CEP135 Splice Isoform Controls Centriole Duplication. Current Biology. 2015; 25: 2591–2596.

[17] Sha Y, Xu X, Mei L, Li P, Su Z, He X, *et al*. A homozygous CEP135 mutation is associated with multiple morphological abnormalities of the sperm flagella (MMAF). Gene. 2017; 633: 48–53.

[18] Yang Y, Chen M, Li JR, Hong RJ, Yang J, Yu F, *et al*. A cilium-independent role for intraflagellar transport 88 in regulating angiogenesis. Science Bulletin. 2020; 66: 727–739.

[19] Guedez L, Stetler-Stevenson WG. Directed In Vivo Angiogenesis Assay (DIVAA) for the Screening of Angiogenesis Modulators. Springer: Netherlands. 2012.

[20] Livak KJ, Schmittgen TD. Analysis of relative gene expression data using real-time quantitative PCR and the 2(-Delta Delta C(T)) Method. Methods (San Diego, Calif.). 2001; 25: 402–408.

[21] Gao J, Huo L, Sun X, Liu M, Li D, Dong J, *et al*. The tumor suppressor CYLD regulates microtubule dynamics and plays a role in cell migration. The Journal of Biological Chemistry. 2008; 283: 8802–8809.

[22] Shi X, Liu M, Li D, Wang J, Aneja R, Zhou J. Cep70 contributes to angiogenesis by modulating microtubule rearrangement and stimulating cell polarization and migration. Cell Cycle. 2012; 11: 1554–1563.

[23] Shakhov AS, Alieva IB. The Centrosome as the Main Integrator of Endothelial Cell Functional Activity. Biochemistry. Biokhimiia. 2017; 82: 663–677.

[24] Hussain MS, Baig SM, Neumann S, Nürnberg G, Farooq M, Ahmad I, *et al*. A truncating mutation of CEP135 causes primary microcephaly and disturbed centrosomal function. American Journal of Human Genetics. 2012; 90: 871–878.

[25] Sonnen KF, Schermelleh L, Leonhardt H, Nigg EA. 3D-structured illumination microscopy provides novel insight into architecture of human centrosomes. Biology Open. 2012; 1: 965–976.

[26] Singh P, Ramdas Nair A, Cabernard C. The centriolar protein Bld10/Cep135 is required to establish centrosome asymmetry in Drosophila neuroblasts. Current Biology. 2014; 24: 1548–1555.

[27] Kraatz S, Guichard P, Obbineni JM, Olieric N, Hatzopoulos GN, Hilbert M, *et al*. The Human Centriolar Protein CEP135 Contains a Two-Stranded Coiled-Coil Domain Critical for Microtubule Binding. Structure. 2016; 24: 1358–1371.

[28] Inanç B, Pütz M, Lalor P, Dockery P, Kuriyama R, Gergely F, *et al*. Abnormal centrosomal structure and duplication in Cep135-deficient vertebrate cells. Molecular Biology of the Cell. 2013; 24: 2645–2654.

[29] Li D, Xie S, Ren Y, Huo L, Gao J, Cui D, *et al*. Microtubule-associated deacetylase HDAC6 promotes angiogenesis by regulating cell migration in an EB1-dependent manner. Protein & Cell. 2011; 2: 150–160.

[30] Zheng Y, Dong Y, Si S, Zhen Y, Gong J. IMB5476, a novel microtubule inhibitor, induces mitotic catastrophe and overcomes multidrug resistance in tumors. European Journal of Pharmacology. 2022; 919: 174802.